Deep-Sea Research, Vol. 28A, No. 7, pp. 665 to 682, 1981.
Printed in Great Britain.

0198-0149/81/070665-18 $02.00/0

The effect of continental shelves on tides

ALLAN J. CLARKE* and DAVID S. BATTISTI*

(*Received* 21 *March* 1980; *in revised form* 2 *October* 1980; *accepted* 15 *December* 1980)

Abstract—Coastal tides are influenced by several factors and one of the most important of these is the character of the adjacent continental shelf. A continental margin theory is derived and used to discuss several different aspects of the effect "smooth" continental shelves have on tides. The main results are as follows. (a) The theory suggests, in accordance with observations, that semi-diurnal tides should be amplified on wide shelves in mid and low latitudes, but that diurnal tides should not be amplified. (b) Continental shelf tidal resonance occurs when the shelf scale $g\alpha/(\omega^2 - f^2)$ (α = shelf bottom slope, ω = tidal frequency) is approximately equal to the shelf width. Theoretical arguments and observation can be used to show that shelf resonance occurs, for example, along sections of the northwest Australian shelf. (c) Given the easily obtained coastal tide, theory shows that tides over the continental shelf and slope can be approximately estimated analytically. Calculations using simple prediction formulae can be made on a hand calculator. Subject to some restrictions, a simple and inexpensive method is thus available for estimating barotropic tides on continental shelves. (d) An appropriate boundary condition for global numerical tidal models, which cannot resolve the continental margin region, is derived. For the diurnal tides, the boundary condition can be well approximated by an impermeable wall condition at the deep-sea continental slope boundary. For the semi-diurnal tides, the impermeable wall condition usually, but not always, suffices; it can break down on wide continental shelves.

1. INTRODUCTION

THE INFLUENCE of continental shelves on barotropic tides can be dramatic. On the wide Patagonian shelf off Argentina, for example, M_2 coastal tidal amplitudes in excess of 3.5 m are observed. This amplitude is many times that typical in the deep ocean. While amplification of semi-diurnal tides on wide shelves seems to generally occur, diurnal tides are rarely strongly amplified. Why should this be so? How wide should a shelf be before significant semi-diurnal amplification occurs? As continental shelves apparently can strongly affect the tides, what deep-sea boundary condition should global numerical tidal models, which cannot resolve the boundary topography, use? These questions have formed the prime motivation for the research presented in this paper.

Some research on the influence of continental shelves on tides has been carried out previously, most notably by FLEMING (1938), REDFIELD (1958), MUNK, SNODGRASS and WIMBUSH (1970), and MILES (1972). Redfield showed that, for the M_2 tide on the east coast of the United States, there is a correlation between shelf width and the coastal tide, with tidal amplitudes generally increasing as the shelf width increases. He also, in effect, suggested that the amplification of the tide across the shelf could be described by the canal theory method of STERNECK (1915). FLEMING (1938) used a similar theory in describing the

* Department of Oceanography, University of Washington, Seattle, WA 98195, U.S.A.

tidal elevations in the Gulf of Panama. However, as the theory later in this paper shows, longshore gradients and rotation, which are omitted by canal theory, are, in general, important for describing tides on continental shelves.

More recent studies by MILES (1972) and MUNK *et al.* (1970) have taken rotation and longshore gradients into account. Miles examined the effect of continental shelf topography on a deep-sea Kelvin wave propagating along the coastline. Munk summarized possible wave motions on continental shelves and used measurements and theory to construct, with some success, the deep-sea tidal response near the California coast. However, they did not specifically address the questions raised earlier.

In this paper, a different approach is adopted. The boundary layer theory describing the approach is presented in Section 2. In following sections the theory is used and in some cases developed further, to discuss the amplification of tides on continental shelves (Section 3), to estimate tides on continental shelves quantitatively (Section 4), and to derive a deep-sea boundary condition for global numerical tidal models (Section 5).

2. A THEORY FOR TIDAL MOTIONS ON CONTINENTAL MARGINS

Because motions on the continental shelf and slope regions only will be considered, direct tidal generation by the large-scale astronomical forcing will be ignored. Under this approximation, the Laplace tidal equations, with frictional effects included, are

$$u_t - fv = -g\eta_x - \frac{\tau_B^x}{\rho H} \tag{2.1}$$

$$v_t + fu = -g\eta_y - \frac{\tau_B^y}{\rho H} \tag{2.2}$$

$$\eta_t + (Hu)_x + (Hv)_y = 0. \tag{2.3}$$

In these equations x and y refer to Cartesian coordinate axes, the x axis pointing perpendicularly away from the coast and the y axis alongshore. The symbols u, v, τ_B^x, τ_B^y, t, f, ρ, g, η, and H refer, respectively, to the velocities in the x and y directions, the bottom friction in the x and y directions, time, the Coriolis parameter, the water density, the acceleration due to gravity, the deviation of the sea surface from its undisturbed level, and the water depth.

The importance of frictional effects is measured by the ratio of the stress terms in (2.1) and (2.2) to the left hand side of these equations. Using the bulk formula to estimate the stresses, the magnitude of the ratio is

$$\frac{c_D|\mathbf{u}|}{H\omega},$$

where c_D is the drag coefficient and ω is the angular frequency of the tide. Clearly friction becomes more and more important as the coast is approached and $H \to 0$. Taking typical values $c_D = 2 \times 10^{-3}$, $|\mathbf{u}| = 0.1\ \mathrm{m\ s^{-1}}$, $\omega = 10^{-4}\ \mathrm{s^{-1}}$, the depth at which the ratio becomes 1 is 2 m. Even if $|\mathbf{u}| = 1\ \mathrm{m\ s^{-1}}$, frictional effects are still only important in depths shallower than 20 m. More detailed measurements support these depth estimates (MAY, 1979). In the following work, it will be assumed that the small volume of water in the frictional boundary layer adjacent to the coast does not strongly affect tidal motions in the

larger volume on the main part of the shelf. Mathematically, this means that τ_B^x and τ_B^y will be ignored in (2.1) and (2.2).

With friction neglected, eliminating all variables in (2.1) to (2.3) in favor of η gives

$$\eta_{xxt}+\eta_{yyt}+\frac{H_x}{H}(f\eta_y+\eta_{xt})+\frac{H_y}{H}(\eta_{yt}-f\eta_x)-\left(\frac{\partial^2}{\partial t^2}+f^2\right)\frac{\eta_t}{gH}=0. \tag{2.4a}$$

Now the longshore (y) scale of the tidal motion on continental margins is principally determined by the y scale in the deep sea [which is 0(2000 km), much greater than typical shelf widths] and also by longshore variations in topography and coastline. Many of the world's continental margins are "smooth" in the sense that their coastlines are quasi-straight (i.e., significant bends in the coastline have a scale much greater than the shelf width) and their longshore variations in shelf topography are much smaller than offshore (x) variations. For these "smooth" continental margins one can write (2.4a) as

$$\eta_{xxt}+\frac{H_x}{H}(f\eta_y+\eta_{xt})-\left(\frac{\partial^2}{\partial t^2}+f^2\right)\frac{\eta_t}{gH}=0 \tag{2.4b}$$

to within a small error determined by the ratio of the second and fourth terms of the left hand side of (2.4a) with the third. Employing the tidal and boundary layer results,

$$\frac{\partial}{\partial t}\gtrsim f,\frac{\partial}{\partial x}\gtrsim\frac{\partial}{\partial y},$$

the error ratio is

$$\lesssim\frac{H}{H_x}\frac{1}{y\text{ scale}}\lesssim\frac{\text{shelf width}}{y\text{ scale}}=\varepsilon.$$

Proceeding further by defining the complex function l as

$$il(x,y)=\frac{\partial\eta}{\partial y}\cdot\eta^{-1}, \tag{2.5}$$

one has that (2.4a) can be written

$$\eta_{xx}+\frac{H_x}{H}\eta_x+\left(\frac{\omega^2-f^2}{gH}+\frac{fl}{\omega}\frac{H_x}{H}\right)\eta=0, \tag{2.6}$$

where $\partial/\partial t$ has been taken to be $i\omega$ because tidal motions are harmonic in time. Note that it can be shown *a posteriori* (see Appendix A) that on the continental margin l is independent of x to within an error of order ε. Thus, l may consistently be taken to be independent of x in (2.6).

In solving (2.6) a stick profile will be used to approximate the continental margin topography (see Fig. 1). For an n segment profile one has

$$H(x)=\alpha_j(x-\beta_j)\qquad a_{j-1}<x\leqslant a_j, \tag{2.7a}$$

where

$$\beta_j=\left\{\begin{array}{ll}0 & j=1\\ \left[a_{j-1}-\sum_{i=1}^{j-1}\frac{\alpha_i}{\alpha_j}\left(a_i-a_{i-1}\right)\right] & j=2,3,\ldots n.\end{array}\right\} \tag{2.7b}$$

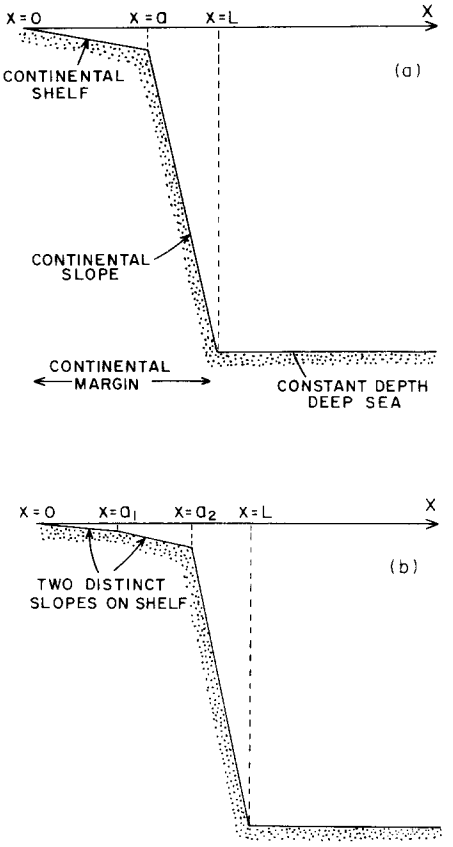

Fig. 1. The simple continental margin profile used in calculating solutions.

Under this "stick" topography approximation and other approximations discussed in the previous paragraph (2.6) can be written

$$\eta_{xx}+\frac{\eta_x}{x-\beta_j}+\mu_j\frac{\eta}{x-\beta_j}=0, \tag{2.8a}$$

where μ_j is the constant

$$\frac{\omega^2-f^2}{g\alpha_j}+\frac{fl}{\omega} \tag{2.8b}$$

with α_j = constant bottom slope for the jth stick of the profile. At the junction of the bottom slopes, the continuity of sea level and velocity perpendicular to the coast demand that η and η_x are continuous. At the coast, η must be finite. These boundary conditions and (2.8) can be used to obtain barotropic sea levels and currents on continental shelf and slope regions given the easily obtained sea levels at the coast.

Solution for a simple shelf profile

Consider a simple shelf and slope geometry, namely that shown in Fig. 1a, and focus on the shelf region $0 \leqslant x \leqslant a$. The solution of (2.8), which is finite at the coast, can be written

in terms of zero-order Bessel functions, or more conveniently,

$$\eta(x) = \eta(0) \sum_{n=0}^{\infty} \frac{(-\mu_1 x)^n}{(n!)^2}. \tag{2.9}$$

Because, typically, μ_1^{-1} runs between roughly 300 and 1000 km, over continental shelves $\mu_1 x \lesssim 1$. Thus (2.9) is rapidly convergent. In fact, in most cases a linear approximation in x is sufficient. This approximation will be used in the remainder of this section, the more general case being treated in Section 3 where tidal amplification is discussed.

When the linear approximation is made, a particularly simple solution is obtained, namely,

$$\frac{\eta(x)}{\eta(0)} = 1 - \left(\frac{\omega^2 - f^2}{g\alpha_1} + \frac{fl_r}{\omega} + \frac{ifl_i}{\omega}\right) x, \tag{2.10}$$

where l_r and l_i denote the real and imaginary parts of l, respectively. Consistent with the linear approximation, this equation can be written in the form

$$\frac{\eta(x)}{\eta(0)} = \left[1 - \left(\frac{\omega^2 - f^2}{g\alpha_1} + \frac{fl_r}{\omega}\right) x\right] \exp\left(\frac{-ifl_i x}{\omega}\right) \tag{2.11}$$

so that $fl_i x/\omega$ is the phase variation across the shelf and

$$\left[1 - \left(\frac{\omega^2 - f^2}{g\alpha_1} + \frac{fl_r}{\omega}\right) x\right]$$

measures the ratio of shelf and coastal amplitudes. Note that because l is independent of x, it can be determined from coastal observations. For $\eta(0) = Ae^{iG}$, one has, by (2.5)

$$l_r = \frac{\partial G}{\partial y} \approx \frac{\Delta G}{\Delta y}, \; l_i = \frac{-\partial A}{\partial y} A^{-1} \approx -\frac{\Delta A}{\Delta y} \frac{1}{A}. \tag{2.12}$$

Thus, l_r and l_i can, in principle, be determined by finite differences along the coast from known coastal values. In practice, noise makes determination of l_r and l_i difficult (see a discussion in Appendix B).

Finally, when the linear approximation is possible (2.10) implies that the currents on the shelf take the simple forms

$$u = \frac{-\eta i\omega}{\alpha_1}, \qquad v = \left(\frac{f}{\alpha_1} - \frac{lg}{\omega}\right)\eta. \tag{2.13}$$

Solution on the continental slope

The solution over the continental slope is of the form

$$\eta(x) = c_1 \sum_{n=0}^{\infty} \frac{[-\mu_2(x-\beta_2)]^n}{(n!)^2} + c_2 F[\mu_2(x-\beta_2)], \tag{2.14}$$

where c_1 and c_2 are constants and

$$F[\mu_2(x-\beta_2)] = \left[\sum_{n=0}^{\infty} \frac{[-\mu_2(x-\beta_2)]^n}{(n!)^2}\right] \ln[\mu_2(x-\beta_2)] + \sum_{n=1}^{\infty} a_n[\mu(x-\beta_2)]^n \tag{2.15}$$

$$a_1 = 2, a_2 = \frac{-3}{4}, a_3 = \frac{11}{108}, \ldots$$

Because of the large bottom slope over the continental slope, $\mu_2 \approx fl/\omega$ and $\mu_2(x-\beta_j)$ are therefore generally small enough that the linear solution in x suffices. In fact, to be consistent with the omission of η_{yy} from (2.6) only the linear solution should be used. Applying the matching conditions at the shelf–slope boundary ($x = a$) determines c_1 and c_2 and gives, for the solution over the slope,

$$\frac{\eta(x)}{\eta(0)} = 1 - \left(\frac{\omega^2 - f^2}{g\alpha_1}\right) a. \left[1 + \frac{\alpha_1}{\alpha_2}\left[\frac{x-a}{a} + \left(1 - \frac{\alpha_1}{\alpha_2}\right) \ln\left\{1 + \frac{\alpha_2}{\alpha_1}\left(\frac{x}{a} - 1\right)\right\}\right]\right] - \frac{flx}{\omega}, \tag{2.16}$$

where

$$\left\{1 + \frac{\alpha_2}{\alpha_1}\left(\frac{x}{a} - 1\right)\right\} = \frac{H(x)}{H(a)},$$

the ratio of the depth at x to that at the shelf break.

For a more general case, when the shelf is clearly broken into two distinct slopes (e.g., the shelf region off Georgia, U.S.A.) a similar analysis to that above gives, for the solution over the slope (see Fig. 1b),

$$\frac{\eta(x)}{\eta(0)} = 1 - \frac{\omega^2 - f^2}{g\alpha_1} a_1 \left\{1 + \frac{\alpha_1}{\alpha_2}\left[\frac{a_2}{a_1} - 1 + \left(1 - \frac{\alpha_1}{\alpha_2}\right) \ln\left(\frac{H(a_2)}{H(a_1)}\right)\right] + \frac{\alpha_1}{\alpha_3}\left[\frac{x-a_2}{a_1} + \left(\frac{a_2 - \dfrac{H(a_2)}{\alpha_3}}{a_1}\right) \ln\left(\frac{H(x)}{H(a_2)}\right)\right]\right\} - \frac{flx}{\omega}. \tag{2.17}$$

MILES (1972) obtained a result similar to (2.16) and (2.17) with more general shelf topography, but for the special case of a deep-sea Kelvin wave. J. HUTHNANCE (personal communication) has recently obtained a version of (2.16) for general shelf topography $H(x)$ [the second term of (2.16) is replaced by

$$-\frac{(\omega^2 - f^2)}{g}\left[\int_0^x \frac{x\,dx}{H}\right].$$

However, the results for general shelf topography and the simplified shelf geometry of Fig. 1 do not differ significantly. Because of this and the ease of application of (2.16) and (2.17) the simplified shelf topography results will be used here in estimating deep-sea levels from coastal ones (see Section 4).

3. TIDAL AMPLIFICATION ON CONTINENTAL SHELVES

The possibility of tidal amplification on continental shelves has been discussed by others, e.g., REDFIELD (1958), MUNK *et al.* (1970), WEBB (1973a,b, 1976), and BUCHWALD (1980). In this section, some general criteria for amplification are discussed and related to observation. In obtaining the criteria, μx cannot be taken to be small and the linearized theory of Section 2 therefore cannot be used. Consequently, the general case is treated below.

(a) *Theory*

Consider the shelf shown in Fig. 1a again, but in this case the solution (2.9) on the shelf need not be linear. Define

$$\lambda = -\frac{a}{\eta(a)} \cdot \frac{\partial \eta}{\partial x}\bigg|_{x=a} = -\frac{\sum_{n=1}^{\infty} \frac{(-\mu a)^n}{(n!)^2} \cdot n}{\sum_{n=0}^{\infty} \frac{(-\mu a)^n}{(n!)^2}}. \tag{3.1}$$

A patching analysis similar to that in Section 2 gives

$$\frac{\eta(x)}{\eta(a)} = 1 - \frac{fl}{\omega}(x-a) - \lambda \frac{\alpha_1}{\alpha_2}\left[\frac{x-a}{a} + \ln\left\{\frac{H(x)}{H(a)}\right\}\right] + 0\left[\left(\frac{\alpha_1}{\alpha_2}\right)^2 ; \frac{\alpha_1}{\alpha_2}\mu_2 x \ln\left\{\frac{H(x)}{H(a)}\right\} ; (\mu_2 x)^2\right]. \tag{3.2}$$

In obtaining (3.2) use was made of the approximation, $\mu_2 \approx fl/\omega$, which follows because the continental slope, α_2, to the deep sea is so large. The large slope also implies that the last term on the right hand side of (3.2) is negligible.

Equation (3.2) can be put into a more explicit form. Use of (3.1) in (3.2) gives

$$\frac{\eta(x)}{\eta(0)} = \left[1 - \frac{fl(x-a)}{\omega}\right]\frac{\eta(a)}{\eta(0)} + \frac{\partial \eta}{\partial x}\bigg|_{x=a} [\eta(0)]^{-1}\, a \frac{\alpha_1}{\alpha_2}\left[\frac{x-a}{a} + \ln\left\{\frac{H(x)}{H(\alpha)}\right\}\right]$$

or, using (2.9)

$$\frac{\eta(x)}{\eta(0)} = \sum_{n=0}^{\infty} \frac{(-\mu_1 a)^n}{(n!)^2}\left[1 - \frac{fl(x-a)}{\omega} + n\frac{\alpha_1}{\alpha_2}\left(\frac{x-a}{a} + \ln\left\{\frac{H(x)}{H(a)}\right\}\right)\right], \tag{3.3}$$

which is the wide-shelf equivalent of (2.16). At $x = L$ one has

$$\frac{\eta(0)}{\eta(L)} = \left\{\sum_{n=0}^{\infty} \frac{(-\mu_1 a)^n}{(n!)^2}\left[1 - \frac{fl(L-a)}{\omega} + \frac{n\alpha_1}{\alpha_2}\left(\frac{L-a}{a} + \ln\left\{\frac{H(L)}{H(a)}\right\}\right)\right]\right\}^{-1}, \tag{3.4}$$

this being an explicit expression for the amplification of the deep-sea tides across the shelf and slope.

For simplicity, consider the case when $l = 0$. Then, as shown in Fig. 2, the amplification

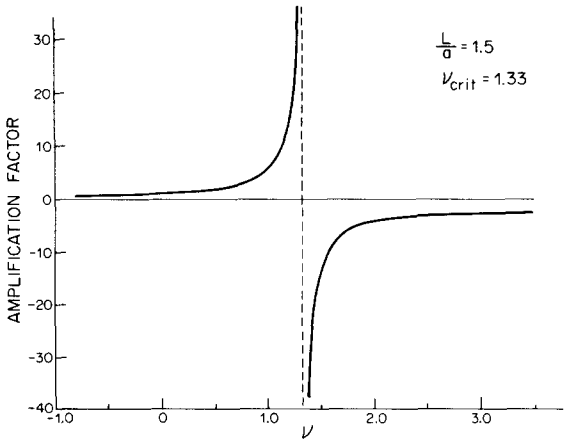

Fig. 2. A plot of the amplification factor $\eta(0)/\eta(L)$ at $l = 0$ against ν for the realistic parameter values $H(a) = 200\,m$, $H(L) = 4$ km, $L/a = 1.5$ (giving $\alpha_1/\alpha_2 = 0.0263$). The plots for $L/a = 1$ and $L/a = 2$ are similar except that the point of resonance is shifted from $\nu_{crit} = 1.33$ to $\nu_{crit} = 1.45$ and 1.19, respectively.

factor increases monotonically from a value 1 to infinity as

$$(\mu a)_{l=0} = \frac{\omega^2 - f^2}{g\alpha_1} \cdot a = \nu$$

increases from zero to a value ν_{crit} such that

$$\sum_{n=0}^{\infty} \frac{(-\nu)^n}{(n!)^2} \cdot \left[1 + \frac{\eta\alpha_1}{\alpha_2}\left(\frac{L-a}{a} + \ln\left\{\frac{H(L)}{H(a)}\right\}\right)\right] = 0. \tag{3.5}$$

At $\nu = \nu_{crit}$ the coastal tide is infinite, i.e., continental shelf tidal resonance occurs. For realistic values of α_1/α_2 and $H(L)/H(a)$, Fig. 2 shows that resonance occurs for $\nu \simeq 1$, i.e., the natural cross-shelf scale, $g\alpha/(\omega^2 - f^2) \simeq a$, the width of the shelf. When $\nu < 0$, the left hand side of (3.5) is always > 1 and amplification never occurs. The physical reason for this is that when $\mu a < 0$ and $l = 0$, wave motions propagating perpendicular to the coast are not possible and therefore constructive interference leading to amplification cannot occur. Finally, although the discussion has focused on $l = 0$, away from resonance one expects to see qualitatively the same amplification behavior for non-zero l. This is due to the fact that away from resonance the boundary layer result, $|fl L/\omega| \lesssim 0.1$, implies that the amplification factor (3.4) is nearly the same in the zero and non-zero l cases.

(b) *Comparison with observation*

Coastal tidal amplitudes are influenced by several factors including the character of the adjacent shelf, the nearby deep-sea tidal amplitude, and irregularities in the coastline and bottom topography. Strongest amplification on smooth shelves seems to occur because of the adjacent shelf. This is borne out in a plot of coastal tidal amplitudes for the M_2 and K_1 tides against

$$\nu = \frac{\omega^2 - f^2}{g\alpha} \cdot a = \frac{\omega^2 - f^2}{gH(a)} \cdot a^2$$

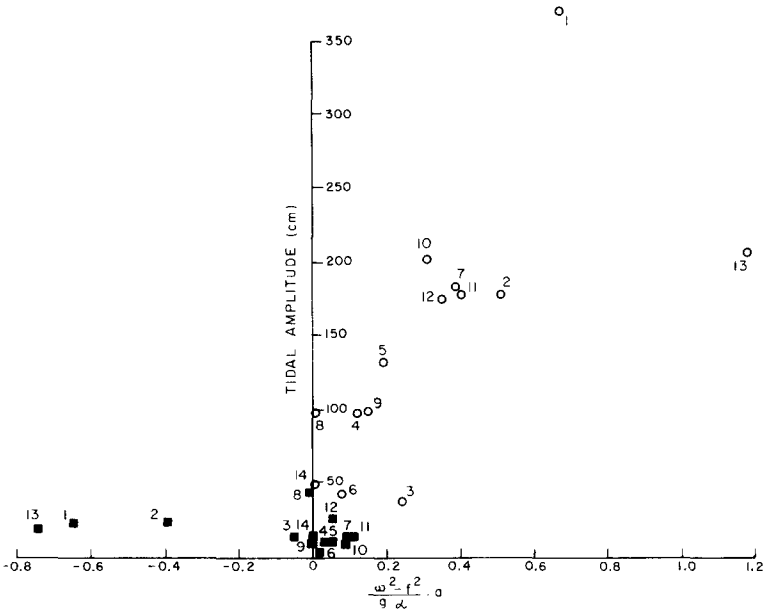

Fig. 3. M_2 and K_1 amplitudes plotted against $(\mu a)_{l=0} = (\omega^2 - f^2) \cdot a/g\alpha = \nu$, where α is the shelf slope; α was crudely estimated by 200m/a, where a is the distance (m) from the coast to the 200-m isobath. Open circles on the graph correspond to M_2 amplitudes, closed squares to K_1 amplitudes. The numbers correspond to the various locations listed in Table 1.

for several stations in various parts of the world. The results (Fig. 3) are qualitatively consistent with theory. Firstly, there is a tendency for larger amplitudes as ν increases. Secondly, no amplification is evident in the left half of the graph where $\nu < 0$. In connection with these results, note the following general trends in coastal tides for smooth shelves: (i) Since ν increases like $(\omega^2 - f^2)\, a^2$, the largest coastal tides occur on wide shelves (large $a \sim 300$ km) in non-polar latitudes [ω(semi-diurnal) $> f$]. (ii) Because

$$\frac{\omega^2(\text{diurnal tide})}{\omega^2(\text{semi-diurnal tide})} \approx \tfrac{1}{4},$$

ν for the diurnal tide is always negative or small and positive so large coastal amplification of diurnal tides will not occur. This may not be the case for irregular coastlines and topography (see CARTWRIGHT, HUTHNANCE, SPENCER and VASSIE, 1980 and Section 6).

Before concluding this sub-section on tidal amplification, it is appropriate to compare the shelf theory of this paper with canal theory, because canal theory has been used in the past to estimate amplification factors for tides on continental shelves (REDFIELD, 1958; PEARSON, 1975b). As one might expect, canal theory (see e.g., LAMB, 1932, §186) is exactly analogous to non-rotating shelf theory, so that μ is changed from

$$\left(\frac{\omega^2 - f^2}{g\alpha} + \frac{fl}{\omega}\right) \text{ to } \frac{\omega^2}{g\alpha}.$$

Therefore, canal theory predicts a larger ν and hence, usually (depending on fl/ω and

Table 1. Locations used in Fig. 3

1.	Santa Cruz, Argentina	50°07'S	68°25'W
2.	Puerto Deseado, Argentina	47°45'S	65°55'W
3.	Mar del Plata, Argentina	38°03'S	57°33'W
4.	Freetown, Sierra Leone	8°30'N	13°14'W
5.	Conakry, Guinea	9°30'N	13°43'W
6.	Carabane, Senegal	12°33'N	16°41'W
7.	Bissau, Guinea-Bissau	11°52'N	15°35'W
8.	Tofino, Vancouver Island	49°09'N	125°54'W
9.	Tybee Light, Georgia	32°02'N	80°54'W
10.	São Luiz, Brazil	2°31'S	44°17'W
11.	Salinopolis, Brazil	0°37'S	47°21'W
12.	Port Hedland, Australia	20°18'S	118°35'E
13.	Comodoro Rivadavia, Argentina	45°52'S	67°29'W
14.	Sydney, Australia	33°51'S	151°14'E

$\nu \lesssim \nu_{crit}$) larger amplification. This is consistent for the United States east coast analyses by REDFIELD (1958) and PEARSON (1975b), who both found that canal theory gives larger than observed amplification factors for the M_2 coastal tide. In this case, shelf and canal theory results do not differ qualitatively as $\omega^2 \simeq 3.3 f^2$ and fl/ω has little effect on the amplification factor. Great differences between canal and shelf theory results do however occur, especially on wide shelves with $\omega \lesssim f$ (e.g., the M_2 tide in the East Siberian Sea).

(c) *Continental shelf tidal resonance*

An interesting aspect of the theory so far not discussed in detail is continental shelf tidal resonance. As implied by (i) above, resonance is likely to occur on wide shelves in mid and low latitudes. Thus, the northwest Australian shelf and the Patagonian shelf off Argentina, both of which have $\nu \sim 1$ and large coastal tidal amplitudes, are open shelf regions that probably contain sections of coastline where resonance occurs. How can one identify such sections of coastline? Although increased coastal amplitude is a guide, probably a clearer indicator is the phase (G) which, at resonance, changes by a large amount compared to typical longshore phase variations. For example, if $l = 0$ and there were no friction, the phase change at resonance would be 180° since at resonance the right hand side of (3.4) changes sign. In practice, non-zero l and friction give a phase change at resonance of less than 180°, the phase change occurring over small but finite ν. In spite of this, large $\partial G/\partial \nu$ should still be a useful resonance indicator.

As ν is a function of ω, one way to estimate $\partial G/\partial \nu$ at a given location is first to calculate the so called "age" of the tide, namely

$$\frac{G(S_2 \text{ tide}) - G(M_2 \text{ tide})}{\omega(S_2) - \omega(M_2)} \approx \frac{\partial G}{\partial \omega} \tag{3.6}$$

and then, a, f, g, and $H(a)$ are constant for a given location, use

$$\frac{\partial G}{\partial \nu} = \frac{\partial G}{\partial \omega}\frac{\partial \omega}{\partial \nu} = \frac{\partial G}{\partial \omega}\frac{\omega^2 - f^2}{2\omega\nu}. \tag{3.7}$$

Note that (3.7) shows that large $\partial G/\partial \omega$ corresponds to large $\partial G/\partial \nu$ and hence to resonance. WEBB (1973a, b) also argued that large tidal age corresponds to resonance. However, in

general there is a disadvantage in using tidal age as a shelf resonance indicator. The disadvantage arises because shelf resonance occurs over a range of ω wider than the tidal bands (WEBB, 1976). Thus, the extra contribution from $\partial G/\partial\omega$ when the shelf is resonant is not easily detected over the background.

Another approach is to plot the phase G along the coast for a given tide (so ω is constant). Due principally to changes in a and $H(a)$, ν varies along the coast and when it exceeds ν_{crit} a large change in G should be observed. Results of this approach are illustrated in Fig. 4b, which shows plots of M_2 phase and ν along a section of the northwest Australian

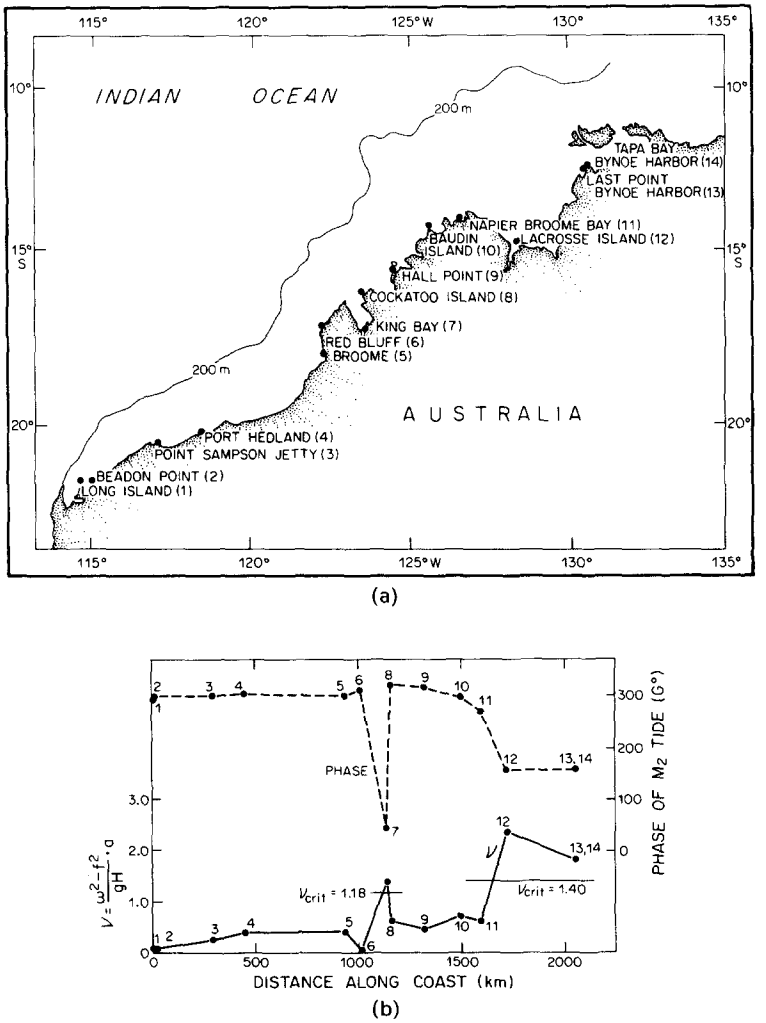

Fig. 4. (a) Tidal stations along the northwest Australian coastline used in Fig. 4b. Note the widening of the shelf at King Bay and Lacrosse Island. (b) ν and phase G of the M_2 tide plotted along the northwest Australian coastline. Sharp changes in G occur when ν_{crit} is exceeded. The numbers on the graph correspond to the numbered locations on the map. Distances refer to a smoothed version of the coastline.

coastline. A large phase change occurs at King Sound and also between Napier Broome Bay and Lacrosse Island. At the latter locations, longshore gradients in phase are two orders of magnitude larger than those associated with usual semi-diurnal gradients. In both these cases the shelf widens considerably (see Fig. 4a) and ν goes from subcritical to supercritical. This indicates that shelf resonance is probably occurring although the theory is not really valid when longshore gradients are large.

The above conclusions concerning resonance assume that the straight coast theory is applicable, at least to a first approximation, to the variable northwest Australian coastline. To test how realistic this assumption is, consider the extreme case near King Sound where about $\frac{1}{3}$ of the shelf is enclosed by land. Canal theory rather than shelf theory would seem to be more appropriate in the sound. However, shelf theory can in fact be used because $\omega^2 \gg f^2$ for the northwest Australian coastline and for this parameter range shelf theory (with $fl/\omega = 0$) and canal theory effectively coincide.

4. A SIMPLE METHOD FOR ESTIMATING TIDES ON CONTINENTAL SHELVES

In the previous section it was shown that simple theory can be used to explain general trends in coastal tidal amplitudes. The theory would be even more useful if, given the readily available tidal measurements at the coast, reasonably accurate estimates of sea levels and currents could be made over the shelf and slope where measurement is comparatively difficult and much more expensive. Early work related to this was done by RATTRAY (1957), who used coastal sea levels to estimate tidal currents near coastlines. Expanding the Laplace tidal equations in a Maclaurin series for small distances from the coast, he obtained reasonable estimates for semi-diurnal currents at Umatilla Reef Light Vessel, three miles from the Washington coast. In this section, the theory of this paper will be checked quantitatively using the few convenient measured deep-sea level values available. The values are given by CARTWRIGHT, ZETLER and HAMON (1979).

Table 2. Data relating to the observed deep-sea tides used in Fig. 5 to compare theory and observation

Location	Depth of measurement	Distance from coast	Data source
30°26′N, 76°25′W (Off Savannah, U.S.A.)	3766 m	450 km	PEARSON (1975b)
48°58′N, 127°17′W (Off Vancouver Island, Canada)	1999 m	82 km	PEARSON (1975a)
32°14′N, 120°51′W (Off San Diego, U.S.A.)	3700 m	282 km	MUNK *et al.* (1970)
39°13′N, 72°10′W (Off New York, U.S.A.)	841 m	178 km	Private communication from Capt. W. V. HALL to CARTWRIGHT *et al.* (1979)
37°01′S, 132°01′E (Off Thevenard, South Australia)	5550 m	490 km	SNODGRASS (1971), IRISH and SNODGRASS (1972)

Results were obtained by hand calculator using the formulae (2.16) and (2.17); l and $\eta(0)$ were estimated from coastal values, but l was difficult to estimate owing to "noise" in the coastal sea-level data and some physical reasoning suggested a smoothing procedure that appears to give better values (see Appendix B).

Calculations of amplitude and phase for the semi-diurnal tides M_2, S_2, and N_2, and amplitude for the diurnal tides K_1 and O_1 were carried out at the five deep-sea stations off Savannah, U.S.A.; Vancouver Island, Canada; San Diego, U.S.A.; New York, U.S.A.; and Thevenard, South Australia (see Table 2). Phase calculations were not performed on the diurnal tides for these tides had considerably smaller longshore slopes* and therefore errors in estimating l were substantially larger. In addition, no phase comparisons were calculated in the South Australian case because there were an insufficient number of stations to estimate l. South Australian amplitude ratios were, however, obtainable using $l = 0$, because these ratios are largely determined by the topographic term $(\omega^2 - f^2)/g\alpha$ rather than fl/ω. Finally, the observed N_2 South Australian coastal amplitude $A(0)$ was very small and a large error in the *observed* ratio $A(x)/A(0)$ seems to have resulted as this ratio was markedly different from the same ratio for tides of similar frequency. [The difference should be $0(\delta\omega/\omega)$ and was instead 0(1).] Consequently, this bad data point was not included.

Results of the afore-mentioned calculations are plotted in Figs 5a, b. If theory and observation were in perfect agreement, all points in each graph in Fig. 5 would lie on a straight line through the origin with slope 45°. As a comparison, the null hypothesis that the sea level in the deep sea is the same as that at the coast is given by the dashed line in each graph. Each graph indicates that the theory is in reasonable agreement with the observation and thus gives significantly better predictions than the null hypothesis. A corollary of the phase results is that it appears that cross-shelf phase differences are probably not due to frictional effects as has been suggested in the past.

5. A DEEP-SEA BOUNDARY CONDITION FOR GLOBAL TIDAL NUMERICAL MODELS

In the preceding sections, attention has been mainly confined to the shelf and slope region. In this section, an important aspect of the deep-sea global tidal problem is considered.

The ocean basins are nearly resonant at tidal frequencies (HENDERSHOTT, 1973; PLATZMAN, 1975, 1978). Consequently, an inaccurate specification of the deep-sea boundary condition can give rise to significantly inaccurate deep-sea tidal predictions. Because of an inability to resolve the continental shelf and slope regions, there has been a difficulty in obtaining a suitable boundary condition at the deep-sea continental slope boundary (HENDERSHOTT, 1976). In view of this, it was decided to use the theory developed in this paper to attempt to justify a useful boundary condition.

* A possible reason for this is that if $l = \omega/\sqrt{gH(L)}$, the ratio of longshore slopes of the diurnal tide (η_1) to the semi-diurnal tide (η_2) is

$$\frac{\partial\eta_1}{\partial y}\Big/\frac{\partial\eta_2}{\partial y} \sim \frac{\omega_1}{\omega_2}\frac{\eta_1}{\eta_2} \doteq \frac{1}{2}\frac{\eta_1}{\eta_2},$$

which is small because generally $|\eta_1/\eta_2| < 1$.

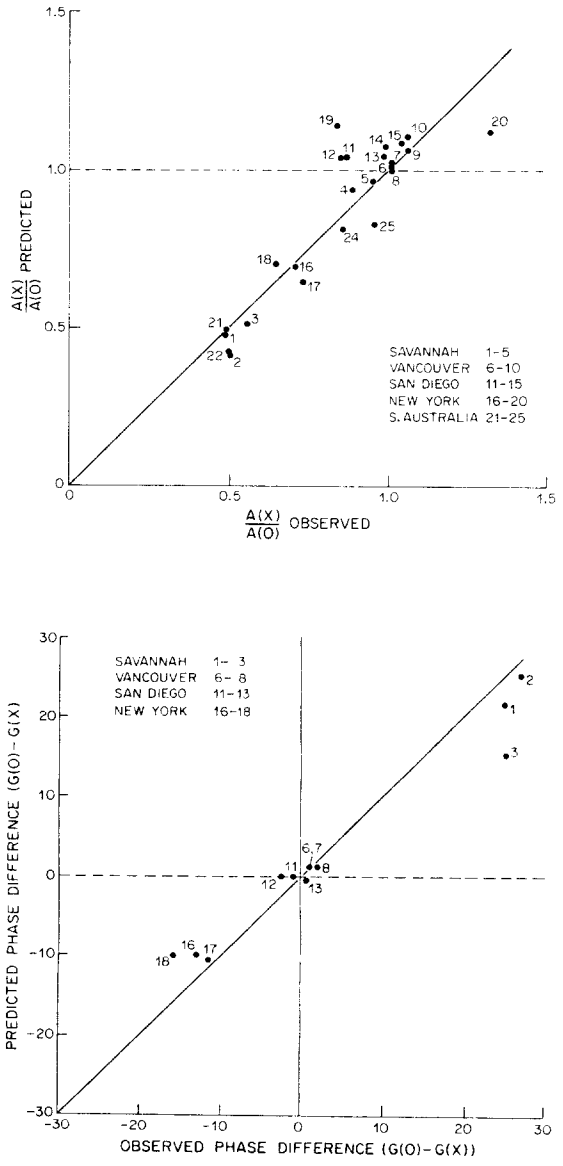

Fig. 5. (a) Predicted ratio of the amplitude at the deep-sea location to that at the coast against the observed ratio. (b) Predicted phase difference between the coast and the deep-sea location plotted against the observed phase difference. In (a) and (b) amplitude ratios and phase differences are plotted in the order M_2, S_2, N_2, and K_1, and O_1. Numbers corresponding to the K_1 and O_1 tides on the phase graph do not appear because l could not be estimated accurately for the diurnal tides. The straight line slope (one) through the origin in each graph denotes the line along which theory and observation are in perfect agreement. The dashed line in each graph corresponds to the null hypothesis that the coastal sea level is the same as that at position x.

Equation (3.2) of Section 3 can be written in the form

$$\frac{\eta(x)}{\eta(a)} = 1 - \frac{fl}{\omega}(x-a) - \lambda_0 \frac{\alpha_1}{\alpha_2}\left[\frac{x-a}{a} + \ln\left\{\frac{H(x)}{H(a)}\right\}\right] + 0\left\{\left(\frac{\alpha_1}{\alpha_2}\right)^2, \frac{\alpha_1}{\alpha_2}\mu_2 x \ln\left\{\frac{H(x)}{H(a)}\right\}, (\mu_2 x)^2\right\}, \tag{5.1}$$

where $\lambda_0 = \lambda|_{l=0}$. Here, the topographic term is retained as for large λ_0 the term can be order (1). Differentiating (5.1) with respect to x gives, at the deep-sea continental slope boundary ($x = L$),

$$\frac{\eta_x(L)}{\eta(a)} = \frac{-fl}{\omega} - \frac{\lambda_0 L}{a^2}\frac{H(a)}{H(L)}\left(1 + \frac{\alpha_1 a}{\alpha_2 L}\right). \tag{5.2}$$

Because, to a first approximation, l is independent of x,

$$il = \frac{\eta_y(L)}{\eta(L)}$$

and so,

$$\eta_x(L)\frac{\eta(L)}{\eta(a)} = \frac{-f\eta_y(L)}{i\omega} - \frac{\lambda_0 L}{a^2}\frac{H(a)}{H(L)}\eta(L)\left(1 + \frac{\alpha_1 a}{\alpha_2 L}\right). \tag{5.3}$$

Using (5.1) applied at $x = L$ in (5.3) and noting $fl(L-a)/\omega \ll 1$ then gives

$$\eta_x(L)\left\{1 - \lambda_0 \frac{\alpha_1}{\alpha_2}\left[\frac{L-a}{a} + \ln\left\{\frac{H(L)}{H(a)}\right\}\right]\right\} = \frac{-f\eta_y(L)}{i\omega} - \frac{\lambda_0 L}{a^2}\frac{H(a)}{H(L)}\eta(L)\left(1 + \frac{\alpha_1 a}{\alpha_2 L}\right). \tag{5.4}$$

As λ_0 is known in terms of ω, f, g, and the bottom slope, (5.4) is a possible boundary condition for global numerical models.

Almost all the world's shelves are such that

$$H(a)/H(L) \approx \frac{1}{20}, \frac{\alpha_1}{\alpha_2} \lesssim \frac{1}{40},$$

and $\lambda_0 \leqslant 1$. $\lambda_0 \leqslant 1$ corresponds to

$$\frac{\omega^2 - f^2}{g\alpha} a = \frac{\omega^2 - f^2}{gH(a)} a^2 \leqslant 0.64.$$

For the semi-diurnal tide this corresponds to $a \leqslant$ about 250 km at the equator, 350 km in mid latitudes, and no restriction near the poles. For the diurnal tide, observed shelf widths are always small enough to give $\lambda_0 \leqslant 1$. For such a parameter range a good approximation to (5.4) is

$$\eta_x + \frac{f\eta_y}{i\omega} = 0 \quad \text{on} \quad x = L,$$

i.e.,

$$u = 0 \quad \text{on} \quad x = L. \tag{5.5}$$

Thus, the impermeable wall condition at the deep-sea continental margin boundary always

applies for the diurnal tide and nearly always for the semi-diurnal tide. In rare cases when the shelf is wide enough so that $\lambda_0 > 1$ for the semi-diurnal tide, the transport onto the shelf and slope is significant and (5.4) rather than (5.5) must be used.

Finally, note that as the ocean basins are so close to resonance, neglected first-order effects could introduce significant errors into a model with boundary condition (5.4). The first-order errors include friction and the more fundamental discrete numerical approximation to the Laplace tidal equations. However, equation (5.4) is the zero-order boundary condition and this should be used before adjusting the numerical solution with a friction parameter.

6. CONCLUDING REMARKS

The main results of this paper are as follows: (1) A simple method for estimating tides on smooth continental margins given the easily obtainable coastal tides has been derived and, to some extent, verified. (2) The accuracy of the application of the simple method is chiefly limited by the necessity of having to calculate longshore gradients from noisy historical coastal sea-level data. Much greater accuracy can probably be obtained by making coastal measurements on open stretches of coastline with present day instruments. (3) A simple lowest order deep-sea boundary condition for global numerical tidal models has been suggested. For the diurnal tide, this boundary condition can be well approximated by an impermeable wall condition at the deep-sea continental slope boundary. For the semi-diurnal tides, the impermeable wall condition usually, but not always, suffices; it breaks down on wide continental shelves. (4) An explanation has been offered for general trends in semi-diurnal and diurnal coastal tidal amplitudes for smooth continental shelves. Criteria for continental margin tidal resonance were derived and crudely verified.

Finally, it should be mentioned that the theory has not taken into account several factors that can result in significantly different dynamics for tides on continental margins. These factors include irregularities in the coastline, the presence of islands near the coast, frictional effects, and steep longshore gradients in the bottom topography. Specific geographic regions, where the present theory does not apply, are in the Bering Sea near the Aleutian Islands (significant bend in the Alaskan coast) and near St. Kilda, where the Outer Hebrides appears to strongly distort the shelf tide. However, the authors feel that the smooth shelf theory can be used on most continental shelves and, in any case, when not applicable, can point to interesting anomalous effects.

Acknowledgements—Both authors would like to thank DON SIMPSON (National Ocean Survey), Capt. STANLEY HUGGETT (Pacific region, Institute of Oceanographic Information, Canada) and PAUL-ANDRÉ BULDUC (Marine Environmental Data Service, Canada) for the coastal tide constants used in Section 4. We would also like to acknowledge helpful advice given by Dr JOHN M. HUTHNANCE, Dr ROBERT HALL and Dr LAWRENCE A. MYSAK. This work was supported by NSF grant OCE79-07042 and represents contribution No. 1197 from the Department of Oceanography, University of Washington, Seattle, WA 98195, U.S.A.

APPENDIX A

Proof that l is effectively independent of x on the continental margin

From the definition of l (equation 2.5), one has

$$i\frac{\partial l}{\partial x} = \frac{\eta\eta_{xy} - \eta_y\eta_x}{\eta^2}. \tag{A1}$$

To fix ideas, consider the case of a wide shelf of constant slope. From equation (2.9)

$$\frac{\partial \eta}{\partial y} = \frac{\partial \eta(0)}{\partial y}\left(\sum_{n=0}^{\infty} \frac{(-\mu x)^n}{(n!)^2}\right)\left(1+0(\varepsilon)\right) \tag{A2}$$

$$\frac{\partial \eta}{\partial x} = -\eta(0)\left(\sum_{n=0}^{\infty} \frac{(-\mu x)^{n-1}}{(n!)^2} \cdot n \cdot (u_x x+\mu)\right) \tag{A3}$$

$$\frac{\partial^2 \eta}{\partial x \partial y} = -\frac{\partial \eta(0)}{\partial y}\left(\sum_{n=0}^{\infty} \frac{(-\mu x)^{n-1}}{(n!)^2} \cdot n \cdot (\mu_x x+\mu)\right)\left(1+0(\varepsilon)\right). \tag{A4}$$

Substituting the above expressions into (A1) yields $il_x = 0$ to within an error of order ε. A similar method can be used to show l effectively independent of x for the more general topography described in equations (2.7).

APPENDIX B

In many cases, a crucial parameter in obtaining deep-sea tidal values from coastal data is l. As stated in the text, l is independent of x and therefore can, in theory, be calculated from coastal values. However, in practice, estimating longshore slopes in noisy historical coastal data is difficult. The subsequent discussion illustrates the method used in this paper to determine l.

Consider Fig. 6, which shows measured M_2 amplitude and phase plotted with distance along the east coast of the United States. The graphs consist of small-scale perturbations on a slowly varying background. The perturbations, having a scale of the station separation, are probably due to locally irregular coastline and topographic influences or measurement error. As such, the perturbations should not be included in an estimate of l over the shelf and slope. In order to smooth over the "noise" associated with the coastal perturbations an appropriate polynomial can be fitted to the data by least squares. The degree of the polynomial is determined by $2\pi\sqrt{gH(L)}/\omega$, an estimate of the longshore deep-sea wavelength. For example, for the case illustrated in the figure, a quadratic fit was chosen

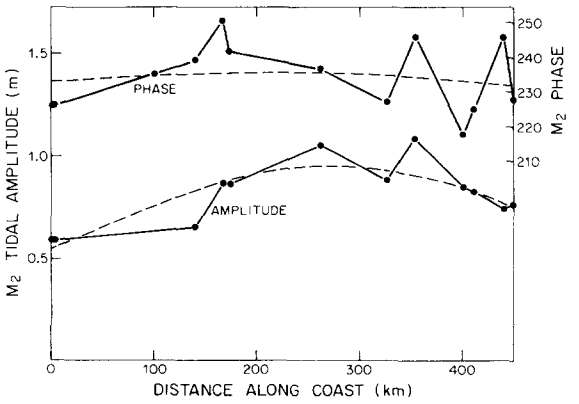

Fig. 6. M_2 amplitude and phase plotted against distance along a section of the east coast of the United States near Savannah. The dashed lines denote the least-squares quadratic fits.

since the distance over which the data were plotted (450 km) was about 1/20 of a wavelength. A lower degree polynomial would not have approximated the signal as well and a higher order polynomial would have begun to include too much "noise". Once the quadratic fit is available, l at the appropriate point along the coast can be calculated using (2.12) of Section 2.

One further point should be made. The smaller amplitude tides have a lower signal-to-noise ratio and therefore estimates of l using the lower amplitude data will, in general, give rise to a larger error. Therefore, it is better to estimate l for all the semi-diurnal and diurnal tides using the largest amplitude tide from each species. This is permissible because tides of the same species have negligibly different l. For

$$l \sim \sqrt{\frac{gH(L)}{\omega}},$$

the error is

$$\frac{\delta l}{l} \sim \frac{\delta\omega}{\omega} \ll 1.$$

REFERENCES

BUCHWALD V. T. (1980) Resonance of Poincaré waves on a continental shelf. *Australian Journal of Marine and Freshwater Research*, **31**, 451–457.

CARTWRIGHT D. E., B. D. ZETLER and B. V. HAMON (1979) *Pelagic tidal constants*. Published by International Association for the Physical Sciences of the Ocean, 65 pp.

CARTWRIGHT D. E., J. M. HUTHNANCE, R. SPENCER and J. M. VASSIE (1980) On the St. Kilda shelf tidal regime. *Deep-Sea Research*, **27**, 61–70.

FLEMING R. H. (1938) Tides and tidal currents in the gulf of Panama. *Journal of Marine Research*, **1**, 192–206.

HENDERSHOTT M. C. (1973) Ocean tides. *Transactions of the American Geophysical Union*, **54**, 76–86.

HENDERSHOTT M. C. (1976) Numerical models of ocean tides. In: *The sea*, Vol. 6, E. D. GOLDBERG, I. N. MCCAVE, J. J. O'BRIEN and J. H. STEELE, editors, Interscience, pp. 47–95.

IRISH J. D. and F. E. SNODGRASS (1972) Australian–Antarctic tides. *American Geophysical Union, Antarctic Research Series*, **19**, 101–116.

LAMB H. (1932) *Hydrodynamics*, 6th Edition, Dover, New York, 738 pp.

MAY P. M. (1979) Analysis and interpretation of tidal currents in the coastal boundary layer. Ph.D. Thesis, Massachusetts Institute of Technology and Woods Hole Oceanographic Institution, 197 pp.

MILES J. W. (1972) Kelvin waves on oceanic boundaries. *Journal of Fluid Mechanics*, **55**, 113–127.

MUNK W., F. SNODGRASS and M. WIMBUSH (1970) Tides offshore: transition from California coastal to deep-sea waters. *Geophysical Fluid Dynamics*, **1**, 161–235.

PEARSON C. A. (1975a) Deep-sea tide and current observations in the Gulf of Alaska and Northeast Pacific. *NOAA Technical Memorandum NOS* 16, 23 pp.

PEARSON C. A. (1975b) Deep-sea tide observations off the southeastern United States. *NOAA Technical Memorandum NOS* 17, 12 pp.

PLATZMAN G. W. (1975) Normal modes of the Atlantic and Indian oceans. *Journal of Physical Oceonography*, **5**, 201–221.

PLATZMAN G. W. (1978) Normal modes of the world ocean. Part I. Design of a finite element barotropic model. *Journal of Physical Oceanography*, **8**, 323–343.

RATTRAY M., JR. (1957) On the offshore distribution of tide and tidal current. *Transactions of the American Geophysical Union*, **38**, 675–680.

REDFIELD A. C. (1958) The influence of the continental shelf on the tides of the Atlantic coast of the United States. *Journal of Marine Research*, **17**, 432–448.

SNODGRASS F. E. (1971) *Eltanin* Cruise 41. *Antarctic Journal of the United States*, **6**, 12–14.

STERNECK R. V. (1915) Hydrodynamische Theorie der halbtägigen Gezeiten des Mittelmeeres. *Sitzungsberichte der Akademie der Wissenschaften in Wien, Mathematisch-naturwissenschaftliche Abt. II a*, **124**, 905–979.

WEBB D. J. (1973a) On the age of the semi-diurnal tide. *Deep-Sea Research*, **20**, 847–852.

WEBB D. J. (1973b) Tidal resonance in the Coral Sea. *Nature, London*, **243**, 511.

WEBB D. J. (1976) A model of continental-shelf resonances. *Deep-Sea Research*, **23**, 1–15.